

Gravitational Wave Signatures of Black Hole Quasinormal Mode Instability

José Luis Jaramillo¹, Rodrigo Panosso Macedo^{2,3,4} and Lamis Al Sheikh^{1,5}

¹*Institut de Mathématiques de Bourgogne (IMB), UMR 5584, CNRS, Université de Bourgogne Franche-Comté, F-21000 Dijon, France*

²*School of Mathematical Sciences, Queen Mary, University of London, Mile End Road, London E1 4NS, United Kingdom*

³*CENTRA, Departamento de Física, Instituto Superior Técnico—IST, Universidade de Lisboa—UL, Avenida Rovisco Pais 1, 1 1049 Lisboa, Portugal*

⁴*STAG Research Centre, University of Southampton, University Road, SO17 1BJ Southampton, United Kingdom*

⁵*Institut de Mathématiques de Marseille (i2m), UMR 7373, CNRS, Université de Aix-Marseille 13453 Marseille Cedex 13, France*

 (Received 9 May 2021; revised 17 January 2022; accepted 3 May 2022; published 26 May 2022)

Black hole (BH) spectroscopy has emerged as a powerful approach to extracting spacetime information from gravitational wave (GW) observed signals. Yet, quasinormal mode (QNM) spectral instability under small scale perturbations has been recently shown to be a common classical general relativistic phenomenon [J. L. Jaramillo *et al.*, *Phys. Rev. X* **11**, 031003 (2021)]. This requires assessing its impact on the BH QNM spectrum, in particular on BH QNM overtone frequencies. We conclude (i) perturbed BH QNM overtones are indeed potentially observable in the GW waveform, providing information on small-scale environment BH physics, and (ii) their detection poses a challenging data analysis problem of singular interest for LISA astrophysics. We adopt a twofold approach, combining theoretical results from scattering theory with a fine-tuned data analysis on a highly accurate numerical GW ringdown signal. The former introduces a set of effective parameters (partially relying on a BH Weyl law) to characterize QNM instability physics. The latter provides a proof of principle demonstrating that the QNM spectral instability is indeed accessible in the time-domain GW waveform, though certainly requiring large signal-to-noise ratios. Particular attention is devoted to discussing the patterns of isospectrality loss under QNM instability, since the disentanglement between axial and polar GW parities may already occur within the near-future detection range.

DOI: 10.1103/PhysRevLett.128.211102

Introduction.—Are *all* black-hole vibrational modes observable in gravitational-wave astronomy? What astrophysical and fundamental physics information do they *actually* convey?

Gravitational waves (GW) from binary systems are systematically observed by current GW antennas [1]. The late-time radiation of newly formed black holes (BHs) is characterized by an exponentially damped, oscillating signal. The quasinormal modes (QNMs) $\omega = \omega^R + i\omega^I$ encode the decaying scales $1/\omega^I$ and oscillating frequencies $|\omega^R|$. An essential tool in astrophysics, fundamental gravitational physics, and mathematical relativity [2–6], QNMs provide structural information about the BH’s background. The future generation of ground- and space-based detectors shall provide data sufficiently accurate to measure several QNMs [7–16], allowing the addressing of fundamental questions in physics [17,18].

Small environmental perturbations are not expected to radically disrupt the underlying BH spacetime, given the confidence in BH dynamical stability. Yet, instabilities seem intrinsic to the theory at the spectral level [19–25]. High-wave-number fluctuations may alter significantly the QNM spectrum [19], with stronger effects in the high overtones [26]. Since recent GW events have opened a rich

discussion on the detectability of overtones and higher harmonic modes [11–13,28–31], addressing our opening questions is paramount for correctly interpreting current and future GW observations.

BH perturbation theory is described via a nonconservative system with energy leaking into the BH and propagating out to the wave zone. Evolution is generated by non-self-adjoint operators, in a common framework across classical and quantum systems [32]. The notion of *pseudospectrum*, recently introduced into gravity [19], allows the identification of spectral instabilities in nonconservative systems [32–35]. As a topographical map, the pseudospectrum contour level with value ϵ delimits the complex plane region where QNMs can migrate when the system undergoes perturbations of order ϵ . Such an ϵ -contour line lies up to a distance $\sim\kappa\epsilon$ of the spectrum, with κ a “conditioning number.” Spectral stability is characterized by $\kappa \sim 1$, whereas instabilities occur for $\kappa \gg 1$. In the latter case, contour lines extend into large complex plane regions. Remarkably, this arises for BHs [19,24,25,36] (see Fig. 1).

QNM instability.—To trigger the instabilities, Ref. [19] introduced an *ad hoc* modification $\epsilon\delta V_k$ ($\epsilon \ll 1$) into the potential governing the dynamics of GWs on a spherically symmetric BH spacetime. When having a sinusoidal profile

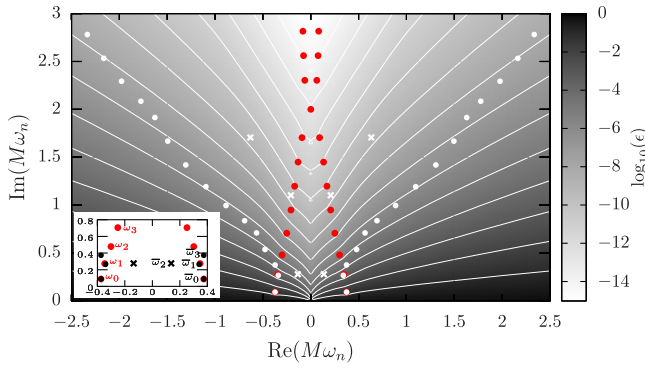


FIG. 1. Schwarzschild spectrum (red circles) and pseudospectrum [$\log_{10}(\epsilon)$ gray scale] for the gravitational $\ell = 2$ modes. The latter captures the norm (a positive number) of the resolvent (essentially, the Green function) of the operator determining the evolution dynamics [19]. The ϵ -pseudospectra contour lines (white) delimit the regions where eigenvalues may move under order- ϵ perturbations of the non-self-adjoint evolution generator. In BH spacetimes, they spread open (ϵ growing downward), signaling spectral instabilities. Under perturbations $\epsilon\delta V_k$ characterized by small amplitude $\epsilon \ll 1$ and moderate-to-large wave number k , the QNM overtones differ significantly from their original values. Generically, one observes that perturbed branches share the pseudospectra’s tendency [19] (white circles). Moreover, internal modes appear (white crosses), with $\omega_{\text{internal}}^I \sim \omega_{\text{branch}}^I$ but $|\omega_{\text{internal}}^R| < |\omega_{\text{branch}}^R|$. The displayed crosses and circles in white arise from a perturbation with parameters $\epsilon = 10^{-3}$ and $k = 10$. The inset shows the first few QNMs with ordering labels obeying $\omega_n^I < \omega_{n+1}^I$.

in the radial direction, $\epsilon\delta V_k$ mimics a Fourier mode from a realistic potential and it captures the contribution of small and large scale perturbations via a wave number k . In particular, the QNM instability discussed here is a large wave number effect [19], starting already at moderate values of k , as illustrated in Fig. 1 showing the overtone instability for $k = 10$. We stress the appearance of (i) branches opening similarly to the pseudospectra lines (white circles), dubbed “Nollert-Price” (NP) branches [22,23] in Ref. [19]; (ii) modes (white crosses) with $|\omega^R| < |\omega_{\text{branch}}^R|$, for $\omega^I \sim \omega_{\text{branch}}^I$, i.e., inside the region bounded by the NP branches, named here “internal modes.”

Specific values for the perturbed QNMs depend on the particular model for the environmental effects or modifications in the gravity theory. Yet, as discussed in Ref. [19], the opening pattern observed in Fig. 1 is rather generic, which raises the need for a research program aiming at understanding the GW observational implications of such QNM instabilities and their universality properties. The challenge lies on several fronts.

On the theoretical side, in the effort to model the specifics of the local environmental astrophysics, or extending gravity beyond general relativity (e.g., [37,38]), GW astronomy shall profit from existing results in the theory of scattering resonances [39–49]. Specifically, theorems permitting us to extract perturbed QNM patterns

reflecting features agnostic to the particular model under consideration. On the data analysis side, one may need enhanced detection pipelines so that the features displayed in Fig. 1 are not overlooked, if present.

In the following three sections, we explore three aspects allowing us to evaluate and characterize QNM instabilities: effective parameters, Weyl law, and isospectrality loss.

Effective parameters.—Consistent with theorems for scattering resonances [39–49], our numerical analysis demonstrates the logarithmic asymptotics of pseudospectra contour lines, $\omega^I \sim C_1 + C_2 \ln(|\omega^R| + C_3)$ for $|\omega^R| \gg 1$, with C_1 , C_2 , and C_3 constants. Asymptotics offer a guideline to identifying the relevant patterns of physical phenomena [50]. In our QNM instability setting, perturbed NP branches open up in the complex plane and approach from above [51] the pseudospectral lines, that define the (upper) boundaries of QNM-free regions. As the size and wave number of C^∞ perturbations increase, QNMs get closer to the pseudospectra lines, so the latter become good proxies of QNM branches. Our results demonstrate that their logarithmic behavior starts actually very close to the unperturbed spectrum (see Supplemental Material [52] and Ref. [36]), enhancing the observable implications.

If the dynamics of the physical scenario is dictated by potentials with discontinuities at some p th derivative (i.e., of class C^p), then the spectra asymptotics reach *exactly* the logarithmic boundaries of the pseudospectra [39,51]. The real ω_n^R and imaginary ω_n^I parts have the asymptotic behavior ($n \gg 1$)

$$\omega_n^R \sim \pm \frac{\pi}{L^R} (n + \tilde{\gamma}), \quad \omega_n^I \sim \frac{1}{L^R} [\gamma \ln(|\omega_n^R| + \gamma') - \ln S], \quad (1)$$

which defines the so-called “Regge QNM branches” [39,51]. Reverberations within chambers with a length scale L^R is the mechanism behind the opening of the spectra into such log-branches [51,53,54]. These are modulated by “regularity” $\gamma, \tilde{\gamma}, \gamma'$ and “strength” S parameters. In particular, Eq. (1) was heuristically observed in low regularity BH-like potentials [22,23,55,56], and neutron stars w modes [54,57,58].

Detecting QNMs obeying Eq. (1) would be a strong indication of an underlying low regularity (C^p) potential. Motivated by such $n \gg 1$ pattern, we introduce here a set of effective parameters, formally evaluated in the limit $n \rightarrow \infty$:

$$L^R := \pi/|\Delta\omega_n^R|, \quad (\text{reverberation length scale}), \quad (2)$$

$$\gamma := L^R \Delta\omega_n^I / \Delta \ln \omega_n^R, \quad (\text{“small-scale” structure}), \quad (3)$$

$$\ln S := \gamma \ln(\omega_n^R) - L^R \omega_n^I, \quad (\text{perturbation strength}). \quad (4)$$

The strict applicability of Eqs. (2)–(4) is constrained to scenarios with nonsmooth (i.e., $C^{p < \infty}$) potentials [51,53,54]. For instance, these definitions directly recover the parameters from the spiked truncated dipole potential [23], namely $L^R \sim x_\delta - x_0$ (length of “cavity”) and $S \sim V_\delta$ (perturbation

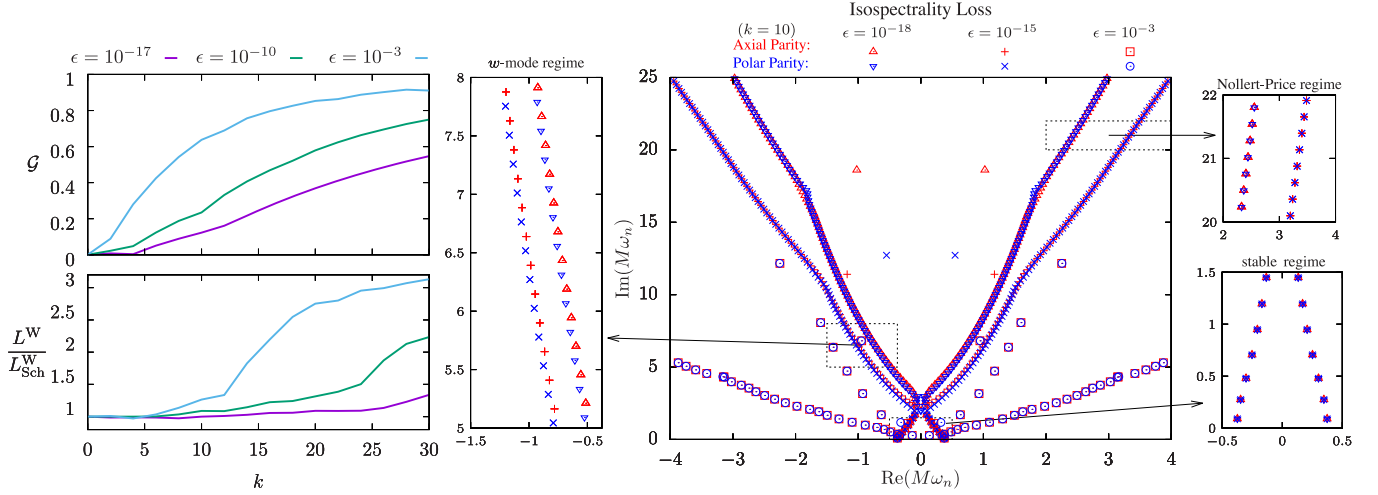


FIG. 2. Left panel: effective measures accounting for QNMs’ distribution. Perturbed potential amplitudes $\epsilon = 10^{-17}, 10^{-10}, 10^{-3}$. Branch opening is assessed by $\mathcal{G} = \lim_{n \rightarrow \infty} \omega_n^R / |\omega_n|$ (top). Schwarzschild QNMs have $\mathcal{G} = 0$, whereas Eq. (1) yields $\mathcal{G} = 1$. The behavior $\mathcal{G} \rightarrow 1$ as $k \rightarrow \infty$ indicates QNMs migrating toward ϵ -pseudospectra log-lines in the large wave number limit. The Weyl law length L^W (bottom) follows from counting the number of QNMs within a delimited region in the complex plane. The transition $L^W/L_{\text{Sch}}^W = 1$ to $\text{O}(3)$ follows from QNMs internal to the branches becoming densely populated. Right panel: isospectrality loss between axial (red) and polar (blue) parities for gravitational $\ell = 2$ modes in Schwarzschild under sinusoidal perturbations $e\delta V_k$ with wave number $k = 10$, $\epsilon = 10^{-18}, 10^{-15}, 10^{-3}$. The insets show the three different regimes with focus on $\epsilon = 10^{-18}, 10^{-15}$. In the stable regime, lower QNMs are not affected by instability, thus axial and polar QNMs differ with order ϵ . The “w-mode” regime strongly distinguishes axial and polar QNMs into an alternating pattern. In the Nollert-Price regime axial and polar QNMs differ again just within order ϵ , despite the wider branch opening. Transition between the regimes occurs close to internal modes. For high ϵ or k the Nollert-Price overtakes the stable and w-mode regimes, as for instance, in the case $\epsilon = 10^{-3}$.

delta-potential amplitude). Furthermore, polytropic neutron stars [57] have $L^R \sim r^*$ (star’s radius), $\gamma \sim \mathcal{N}$ (polytropic index), and $S \sim$ “discontinuity jump of the potential.” Further illustration is found in [51], where the small-scale γ is related to regularity loss. In the case of smooth C^∞ potentials, available rigorous results for the spectra distribution within the ϵ -pseudospectra region are less sharp, but QNMs must always lie above the logarithmic curves [51]. We conjecture that the QNMs reach the log curves in the large k wave number ultraviolet limit.

Supporting this statement, we introduce $\mathcal{G}_n = \omega_n^R / |\omega_n|$ to measure the branch opening. This is a different representation of the so-called quality factor Q_n [59,60]. Schwarzschild QNMs’ asymptotics [61] gives $\mathcal{G} := \lim_{n \rightarrow \infty} \mathcal{G}_n = 0$, whereas Eq. (1) yields $\mathcal{G} = 1$. Realistic BH environments may have an intermediate behavior. Indeed, the upper-left panel in Fig. 2 shows the monotonic increase of $\mathcal{G} \in [0, 1]$ (for several ϵ ’s) with k . The behavior $\mathcal{G} \rightarrow 1$ as $k \rightarrow \infty$ strongly indicates that pseudospectra’s log-boundaries are attained for $k \gg 1$.

Weyl law.—The Weyl law is a spectral concept common across physical theories [62–64], but scantily explored in GW physics [65]. A simple count of modes within a circle in the complex plane provides a typical length scale for the physical problem. More precisely, let $N(\omega)$ be the number of QNMs in the radius $|\omega_n| < \omega$ ($\omega \in \mathbb{R}$). Then, for one-dimensional potentials, the Weyl law states $N(\omega) = 2(L^W/\pi)\omega$, with L^W a length scale of the

potential. In higher dimensions, the law provides a measure for the spacetime dimensionality $d + 1$ via $N(\omega) \sim \omega^d$ [66]. The actual proof from the theory of scattering resonances [51,66–68] relies on scenarios modeled by potentials with compact support or of class C^p . Typical potentials in BH perturbation theory do not satisfy the theorems’ hypotheses.

Here, we show that BH QNMs indeed follow a Weyl law. Schwarzschild QNM asymptotics [61] for an angular mode ℓ yields $N_\ell(\omega) = 8M\omega$, i.e., a scale $L_{\text{Sch}}^W = 4\pi M$. This scale connects with the exploration of BH horizon area quantisation and BH thermodynamics based on QNM asymptotics [65,69–72], with a link to Hawking temperature via $2L_{\text{Sch}}^W = (T_{\text{Hawking}})^{-1}$. Besides, summing $N_\ell(\omega)$ over (ℓ, m) yields $N(\omega) \sim \omega^3$, providing a probe to measure deviations to the effective spacetime dimension by counting QNMs.

Weyl’s law remains valid for perturbed BH potentials and L^W is always robustly defined (lower-left panel in Fig. 2). The changes in L^W are not related to the branch opening. Indeed, we observe $|\Delta\omega_n|$ constant along them. Rather, the apparent “phase transition” with “order parameter” L^W/L_{Sch}^W shifting from 1 to $\text{O}(3)$ results from an increase of internal QNMs.

Isospectrality loss.—Another outcome of the QNM overtone instability is the distinction between axial and polar GW parities. While both QNM spectra coincide for the Schwarzschild BH, parity disentanglement is a natural consequence when the system is slightly perturbed [19]. We observe the existence of three regimes of the

isospectrality loss (Fig. 2): (i) *Stable region*.—Relatively low wave number k and small amplitude ϵ perturbations do not trigger the instability in the first few QNM overtones. The perturbed QNMs with polar-axial parities stay at a distance ϵ from their original values. As a result, isospectrality loss is then of the same order ϵ as the perturbation, i.e., $|\omega_n^{\text{axial}} - \omega_n^{\text{polar}}| \sim C_n(k)\epsilon$ [the function $C_n(k)$ is model dependent; see Supplemental Material [52]]. As ϵ or k increase, the stable behavior is observed by fewer and fewer overtones, eventually reducing only to the fundamental mode. Near-future GW observations shall measure both parities in the fundamental QNM, which may discriminate the mechanisms for the isospectrality loss (e.g., [15,73]). (ii) *Alternating axial/polar w modes*.—Moving to higher overtones, parities drastically separate when QNM instability first occurs. QNMs of different parity place themselves in an alternating pattern along the branch, as neutron star w modes do [3,57]. Isospectrality loss is most accessible here, with BHs as compact star mimickers. We observe $\omega_n^R \sim \ln(\omega_n^I)$, $\omega_n^I \sim n$ [cf. the contrast with Eq. (1)]. As ϵ or k increases, this regime descends in $\text{Im}(\mathbb{C})$ toward the first overtones, eventually overcoming the previous stable region. (iii) *Nollert-Price regime*.—In this third regime, the QNMs migrate further away from unperturbed ones. We observe the branches obeying $\omega_n^I \sim \omega_n^R \sim n$, the QNM instability (assessed by the opening of the branch) is stronger than for alternating w modes. Yet, by studying instances in the range $\epsilon \in [10^{-18}, 10^{-1}]$, we observe the isospectrality loss to be again linear in ϵ , as in the stable regime (i). The mechanism behind this result is unclear. This regime dominates over (i) and (ii) for sufficiently large ϵ or k (e.g., $\epsilon = 10^{-3}$ in Fig. 2).

Interestingly, the transition between the three sectors seems to occur precisely upon appearance of an internal mode. New regimes in far asymptotic regions are not excluded, but their numerical study is challenging. We find internal QNMs to be very parity sensitive. In particular, one may observe internal modes among the first overtones already for a moderate wave number. For instance, the first internal mode in Fig. 1 corresponds to $n = 2$ —the QNM order label follows $\omega_n^I < \omega_{n+1}^I$.

Since QNM instabilities are not restricted to the asymptotic behavior of QNM overtones, novel features might be in the near-future detection range. The next section initiates the discussion from a simple data analysis perspective by measuring the perturbed QNMs within a numerical GW time signal. In the section, *unbarred* and *barred* quantities denote dynamics under the *unperturbed* or *perturbed* potential, respectively.

Data analysis.—Our first goal is to assess whether the time evolution $\phi_{\text{evol}}(t)$ of the corresponding wave equation does contain the perturbed QNMs found in the frequency domain analysis. BH spectroscopy relies on the approximation

$$\phi_{\text{evol}}(t) \approx \phi_{\text{spec}}^N(t), \quad \phi_{\text{spec}}^N(t) = \sum_{n=0}^N \mathcal{A}_n e^{-i\omega_n t}. \quad (5)$$

This expansion is indeed justified for sufficiently late times—but prior to the power-law tails [74]—by Lax-Phillips scattering resonance theory, where expression (5) is understood as an asymptotic resonant expansion [40–42] (see also [47,48,75–78]). However, the unexpected nature of the spectral instability results in Ref. [19] prompts us to perform an independent assessment to rule out possible pathological “artifacts” in the frequency domain calculation. The time-domain scheme underlying Eq. (5) provides precisely such an independent test.

The second goal in this section is to bring attention to the need for enhanced algorithms specifically targeting the QNM instabilities within the waveform. Such data analysis strategies should extend the current detection pipelines processing data from the GW events [7–16], in particular *a priori* QNM spectra distributions employed in Bayesian approaches.

To address these issues from a proof-of-principle perspective, we simulate here an ideal ringdown signal. We solve the usual unperturbed Regge-Wheeler wave equation [53] as well as its perturbed version [19] with $\epsilon = 10^{-3}$ and $k = 10$. The solutions have numerical noise at the machine roundoff error [79]. We use the initial data (ID) referred to as “polynomial” in [76] as they provide a benchmark for the results on the QNM spectral decomposition Eq. (5) according to Refs. [76,77].

Prony’s method [80], an instance of the “harmonic inversion” method, is used to read complex frequencies and amplitudes from a signal modeled by Eq. (5) [81]. Table I compares the “spectral” (frequency domain) QNM values against those from the Prony’s fitting of the time-domain signal [82]. We extract three modes in both unperturbed and perturbed cases, but significant digits are lost on the overtones. In the perturbed case, the third inferred mode is assigned to $\bar{\omega}_3$ due to its remarkable proximity to the respective “theoretically calculated” frequency. Despite the loss in significant digits, the accuracy suffices to distinguish unperturbed from perturbed spectra. The method seems, however, insensitive to the internal mode $\bar{\omega}_2$.

Hence, the perturbed modes on the NP branches are not frequency domain artifacts: they are indeed in the time domain signal and should be measurable in GWs if realistic scenarios trigger the instabilities. However, the presence of internal modes in the time signal has not yet been confirmed. It remains to be assessed whether the internal modes are an artifact or, rather, the particular ID is not efficient to excite them.

To address this issue, we use a semianalytical tool [76,77,83] to measure excitation factors $\bar{\mathcal{A}}_n$. They reveal that the internal mode $\bar{\omega}_2$ is very mildly, but unmistakably, excited (see Supplemental Material [52]): with the employed ID we get $\bar{\mathcal{A}}_2 \sim 10^{-3}$, whereas $\bar{\mathcal{A}}_0 \sim \bar{\mathcal{A}}_1 \sim \bar{\mathcal{A}}_3 \sim 10^{-1}$. Thus, all perturbed QNMs are indeed present in the perturbed GW signal. The fainter signal explains why Prony’s method bypasses this internal mode, while its background noise spoils $\bar{\omega}_1$ ’s and $\bar{\omega}_3$ ’s accuracy. An important open question is whether more realistic ID would excite the internal modes more effectively.

TABLE I. QNMs for unperturbed and perturbed Schwarzschild potentials via Prony’s method. Crosses are QNMs not identified.

Unperturbed potential ($\epsilon = 0, k = 0$)				
QNMs	$M\omega_0$	$M\omega_1$	$M\omega_2$	$M\omega_3$
Spectral	$\pm 0.37367168 - 0.08896231i$	$\pm 0.3467110 - 0.2739149i$	$\pm 0.3010534 - 0.4782770i$	$\pm 0.2515049 - 0.7051482i$
Prony’s Fit	$\pm 0.37367169 - 0.08896232i$	$\pm 0.34670 - 0.27392i$	$\pm 0.302 - 0.48i$	$\times \times \times$
Perturbed potential ($\epsilon = 10^{-3}, k = 10$)				
QNMs	$M\bar{\omega}_0$	$M\bar{\omega}_1$	$M\bar{\omega}_2$	$M\bar{\omega}_3$
Spectral	$\pm 0.37364032 - 0.08898850i$	$\pm 0.3401722 - 0.2648723i$	$\pm 0.1367705 - 0.2761794i$	$\pm 0.3735536 - 0.3723973i$
Prony’s Fit	$\pm 0.37364030 - 0.08898850i$	$\pm 0.342 - 0.266i$	$\times \times \times$	$\pm 0.37 - 0.4i$

Discussion.—Building on the general framework described in Ref. [19], we have focused on the implications of high-wave-number QNM overtone instability for GW astrophysics. Specifically, in this work we have (i) introduced a set of effective parameters ($L^R, \gamma, S, \mathcal{G}$) to characterize perturbed (open) NP BH QNM branches and probe small-scale BH environment physics, (ii) identified different regimes of QNM isospectrality loss and proposed $|\omega_n^{\text{axial}} - \omega_n^{\text{polar}}|$ as an observational marker of the perturbation size ϵ , (iii) found a new class of perturbed “internal QNMs,” signaling the transition between isospectrality loss regimes, (iv) established the logarithmic asymptotics of QNM-free regions (pseudospectrum contour lines) and formulated a conjecture for the high-wave-number limit of Nollert-Price QNM branches to logarithmic Regge QNM branches on QNM-free boundaries, (v) introduced a BH Weyl law (and Weyl scale L^W) probing small scale BH physics and spacetime dimension by counting QNMs, (vi) demonstrated the theoretical capability to disentangle perturbed from unperturbed QNMs from the respective (perturbed and unperturbed) time-domain ringdown signals, in spite of the tiny difference between the waveforms, and (as a challenging counterpart to the latter point) (vii) advocated for the need of developing enhanced data analysis schemes capable to effectively disentangle observational (in contrast to theoretical) perturbed and unperturbed GW ringdown signals and to cope with the effective degeneracy of perturbed QNMs, namely a consequence of the universality [19] of perturbed NP QNM patterns.

Under the assumption that realistic astrophysical scenarios can trigger the described QNM instabilities, the previous points directly impact the future of BH spectroscopy. Assessing whether such an assumption is actually realized is a pressing issue for the correct interpretation of GW observations.

We have focused on high-wave-number QNM overtone instabilities. Other QNM instability mechanisms have been proposed [27]. Distinct mechanisms will inform us on different aspects of BH astrophysics. In particular, in the present overtone setting, the measure of \mathcal{G} and the Weyl length scale L^W are complementary, as they assess the two novel aspects in this type of high-wave-number QNM

instability: \mathcal{G} accounts for the NP branch opening in the complex plane, whereas L^W measures the appearance of internal modes. Beyond BH environment physics, such kind of asymptotic overtone diagnostics could offer a bridge to fundamental gravity physics [84].

We finally stress the timely necessity for liaising the theoretical results on the fundamental aspects of BH perturbation theory with the current efforts to set goals and strategies for the GW missions. Detecting QNM overtones in a noisy signal already imposes a challenging data analysis task when a deterministic underlying spectrum is *a priori* available [11–13, 28–30]. The theoretical prediction of BH QNM instability adds another layer of obstacles, since the perturbed QNM overtone specific values will generically incorporate a stochastic component from (random) small-scale perturbations and only general patterns shall be available. This strongly indicates that only detections with very high signal-to-noise ratios will offer eligible candidates for disentangling BH overtone instabilities. In particular, this defines a challenging but tantalizing case for LISA science, requiring the development of specific data analysis tools to cope with a more intricate parameter degeneracy.

We thank W. Barbe, E. Berti, N. Besset, O. Birnholtz, V. Cardoso, T. Daudé, K. Destounis, E. Gasperin, B. Krishnan, O. Meneses Rojas, B. Raffaelli, O. Reula, D. Sharma, and J. Sjöstrand. We also thank the anonymous referees for their valuable comments and suggestions. This work was supported by the French “Investissements d’Avenir” program through project ISITE-BFC (ANR-15-IDEX-03), the ANR “Quantum Fields interacting with Geometry” (QFG) project (ANR-20-CE40-0018-02), the EIPHI Graduate School (ANR-17-EURE-0002), the Spanish FIS2017-86497-C2-1 project (with FEDER contribution), the European Research Council Grant No. ERC-2014-StG 639022-NewNGR “New frontiers in numerical general relativity,” COST Action CA16104 via the Short Term Scientific Mission grant, STFC Grant No. ST/V000551/1 and the European Commission Marie Skłodowska-Curie Grant No. 843152 (Horizon 2020 programme). The project used Queen Mary’s Apocrita HPC facility, supported by QMUL Research-IT, and CCuB computational resources (Université de Bourgogne).

- [1] R. Abbott *et al.* (LIGO Scientific Collaboration and Virgo Collaboration), GWTC-2: Compact Binary Coalescences Observed by LIGO and Virgo During the First Half of the Third Observing Run, *Phys. Rev. X* **11**, 021053 (2021).
- [2] S. Chandrasekhar, *The Mathematical Theory of Black Holes*, Oxford Classic Texts in the Physical Sciences (Oxford University Press, Oxford, 2002).
- [3] K. D. Kokkotas and B. G. Schmidt, Quasinormal modes of stars and black holes, *Living Rev. Relativity* **2**, 2 (1999).
- [4] H. P. Nollert, Topical review: Quasinormal modes: The characteristic “sound” of black holes and neutron stars, *Classical Quantum Gravity* **16**, R159 (1999).
- [5] E. Berti, V. Cardoso, and A. O. Starinets, Quasinormal modes of black holes and black branes, *Classical Quantum Gravity* **26**, 163001 (2009).
- [6] R. A. Konoplya and A. Zhidenko, Quasinormal modes of black holes: From astrophysics to string theory, *Rev. Mod. Phys.* **83**, 793 (2011).
- [7] E. Berti, V. Cardoso, and C. M. Will, On gravitational-wave spectroscopy of massive black holes with the space interferometer LISA, *Phys. Rev. D* **73**, 064030 (2006).
- [8] O. Dreyer, B. J. Kelly, B. Krishnan, L. S. Finn, D. Garrison, and R. Lopez-Aleman, Black hole spectroscopy: Testing general relativity through gravitational wave observations, *Classical Quantum Gravity* **21**, 787 (2004).
- [9] V. Baibhav, E. Berti, V. Cardoso, and G. Khanna, Black hole spectroscopy: Systematic errors and ringdown energy estimates, *Phys. Rev. D* **97**, 044048 (2018).
- [10] I. Ota and C. Chirenti, Overtones or higher harmonics? Prospects for testing the no-hair theorem with gravitational wave detections, *Phys. Rev. D* **101**, 104005 (2020).
- [11] M. Isi, M. Giesler, W. M. Farr, M. A. Scheel, and S. A. Teukolsky, Testing the No-Hair Theorem with GW150914, *Phys. Rev. Lett.* **123**, 111102 (2019).
- [12] M. Giesler, M. Isi, M. A. Scheel, and S. Teukolsky, Black Hole Ringdown: The Importance of Overtones, *Phys. Rev. X* **9**, 041060 (2019).
- [13] M. Isi, W. M. Farr, M. Giesler, M. A. Scheel, and S. A. Teukolsky, Testing the Black-Hole Area Law with GW150914, *Phys. Rev. Lett.* **127**, 011103 (2021).
- [14] M. Cabero, J. Westerweck, C. D. Capano, S. Kumar, A. B. Nielsen, and B. Krishnan, The next decade of black hole spectroscopy, *Phys. Rev. D* **101**, 064044 (2020).
- [15] E. Maggio, L. Buoninfante, A. Mazumdar, and P. Pani, How does a dark compact object ringdown?, *Phys. Rev. D* **102**, 064053 (2020).
- [16] I. Ota and C. Chirenti, Black hole spectroscopy horizons for current and future gravitational wave detectors *Phys. Rev. D* **105**, 044015 (2022).
- [17] L. Barack *et al.*, Black holes, gravitational waves and fundamental physics: A roadmap, *Classical Quantum Gravity* **36**, 143001 (2019).
- [18] E. Barausse *et al.*, Prospects for fundamental physics with LISA, *Gen. Relativ. Gravit.* **52**, 81 (2020).
- [19] J. L. Jaramillo, R. Panosso Macedo, and L. Al Sheikh, Pseudospectrum and Black Hole Quasinormal Mode Instability, *Phys. Rev. X* **11**, 031003 (2021).
- [20] J. M. Aguirregabiria and C. V. Vishveshwara, Scattering by black holes: A simulated potential approach, *Phys. Lett. A* **210**, 251 (1996).
- [21] C. V. Vishveshwara, On the black hole trail ..., in *Proceedings of the 18th Conference of the Indian Association for General Relativity and Gravitation, Madras, India* (1996), pp. 11–22.
- [22] H. P. Nollert, About the significance of quasinormal modes of black holes, *Phys. Rev. D* **53**, 4397 (1996).
- [23] H. P. Nollert and R. H. Price, Quantifying excitations of quasinormal mode systems, *J. Math. Phys. (N.Y.)* **40**, 980 (1999).
- [24] E. Berti, Instability in black hole vibrational spectra, *Physics* **14**, 91 (2021).
- [25] E. Gasperin and J. L. Jaramillo, Physical scales in black hole scattering pseudospectra: The role of the scalar product, [arXiv:2107.12865](https://arxiv.org/abs/2107.12865).
- [26] Motivated from the present work, an instability of the fundamental QNM based on a “flea on the elephant” mechanism has been proposed in [27].
- [27] M. H. Y. Cheung, K. Destounis, R. P. Macedo, E. Berti, and V. Cardoso, The Elephant and the Flea: Destabilizing the Fundamental Mode of Black Holes, *Phys. Rev. Lett.* **128**, 111103 (2022).
- [28] C. D. Capano, M. Cabero, J. Westerweck, J. Abedi, S. Kasta, A. H. Nitz, A. B. Nielsen, and B. Krishnan, Observation of a multimode quasi-normal spectrum from a perturbed black hole, [arXiv:2201.00822](https://arxiv.org/abs/2201.00822).
- [29] X. J. Forteza and P. Mourier, High-overtone fits to numerical relativity ringdowns: Beyond the dismissed $n = 8$ special tone, *Phys. Rev. D* **104**, 124072 (2021).
- [30] R. Cotesta, G. Carullo, E. Berti, and V. Cardoso, On the detection of ringdown overtones in GW150914, [arXiv:2202.02941](https://arxiv.org/abs/2202.02941).
- [31] M. Isi and W. M. Farr, Revisiting the ringdown of GW150914 (2022).
- [32] Y. Ashida, Z. Gong, and M. Ueda, Non-Hermitian physics, *Adv. Phys.* **69**, 249 (2020).
- [33] L. N. Trefethen, A. E. Trefethen, S. C. Reddy, and T. A. Driscoll, Hydrodynamic stability without eigenvalues, *Science* **261**, 578 (1993).
- [34] L. Trefethen and M. Embree, *Spectra and Pseudospectra: The Behavior of Nonnormal Matrices and Operators* (Princeton University Press, Princeton, NJ, 2005).
- [35] J. Sjöstrand, *Non-Self-Adjoint Differential Operators, Spectral Asymptotics and Random Perturbations*, Pseudo-Differential Operators (Springer International Publishing, New York, 2019).
- [36] K. Destounis, R. P. Macedo, E. Berti, V. Cardoso, and J. L. Jaramillo, Pseudospectrum of Reissner-Nordström black holes: Quasinormal mode instability and universality, *Phys. Rev. D* **104**, 084091 (2021).
- [37] N. Yunes and X. Siemens, Gravitational-wave tests of general relativity with ground-based detectors and pulsar timing-arrays, *Living Rev. Relativity* **16**, 9 (2013).
- [38] S. E. Perkins, N. Yunes, and E. Berti, Probing fundamental physics with gravitational waves: The next generation, *Phys. Rev. D* **103**, 044024 (2021).
- [39] T. Regge, Analytic properties of the scattering matrix, *Nuovo Cimento* **8**, 671 (1958).
- [40] P. D. Lax and R. S. Phillips, A logarithmic bound on the location of the poles of the scattering matrix, *Arch. Ration. Mech. Anal.* **40**, 268 (1971).

- [41] P. D. Lax and R. S. Phillips, Scattering theory, in *Pure and Applied Mathematics*, 2nd ed. (Academic Press, Boston, 1989), Vol. 26.
- [42] B. R. Vainberg, On exterior elliptic problems that depend polynomially on the spectral parameter, and the asymptotic behavior for large values of the time of the solutions of nonstationary problems, *Mat. Sb. (N.S.)* **92**, 224 (1973).
- [43] J. Sjöstrand, Geometric bounds on the density of resonances for semiclassical problems, *Duke Math. J.* **60**, 1 (1990).
- [44] A. Martinez, Resonance free domains for non globally analytic potentials, *Ann. Henri Poincaré* **3**, 739 (2002).
- [45] J. Sjöstrand and M. Zworski, Fractal upper bounds on the density of semiclassical resonances, *Duke Math. J.* **137**, 381 (2007).
- [46] M. Zworski, Resonances in physics and geometry, *Not. Am. Math. Soc.* **46**, 319 (1999), <https://citeseerx.ist.psu.edu/viewdoc/summary?doi=10.1.1.162.2708>.
- [47] M. Zworski, Mathematical study of scattering resonances, *Bull. Math. Sci.* **7**, 1 (2017).
- [48] S. Dyatlov and M. Zworski, *Mathematical Theory of Scattering Resonances*, Graduate Studies in Mathematics (American Mathematical Society, Providence, 2019).
- [49] D. Bindel and M. Zworski, Theory and computation of resonances in 1d scattering, <http://www.cs.cornell.edu/~7Ebindel/cims/resonant1d/>.
- [50] R. W. Batterman, *The Devil in the Details: Asymptotic Reasoning in Explanation, Reduction, and Emergence* (Oxford University Press, New York, 2001).
- [51] M. Zworski, Distribution of poles for scattering on the real line, *J. Funct. Anal.* **73**, 277 (1987).
- [52] See Supplemental Material at <http://link.aps.org/supplemental/10.1103/PhysRevLett.128.211102> for detailed evidences supporting the presented statements.
- [53] T. Regge and J. A. Wheeler, Stability of a Schwarzschild singularity, *Phys. Rev.* **108**, 1063 (1957).
- [54] M. V. Berry, Semiclassically weak reflections above analytic and non-analytic potential barriers, *J. Phys. A* **15**, 3693 (1982).
- [55] W. L. Qian, K. Lin, C. Y. Shao, B. Wang, and R. H. Yue, On asymptotical quasinormal mode spectrum for piecewise approximate effective potential, *Phys. Rev. D* **103**, 024019 (2021).
- [56] H. Liu, W. L. Qian, Y. Liu, J. P. Wu, B. Wang, and R. H. Yue, On an alternative mechanism for the black hole echoes, *Phys. Rev. D* **104**, 044012 (2021).
- [57] Y. J. Zhang, J. Wu, and P. T. Leung, High-frequency behavior of w -mode pulsations of compact stars, *Phys. Rev. D* **83**, 064012 (2011).
- [58] M. V. Berry and K. E. Mount, Semiclassical approximations in wave mechanics, *Rep. Prog. Phys.* **35**, 315 (1972).
- [59] P. Lalanne, W. Yan, K. Vynck, C. Sauvan, and J. Hugonin, Light interaction with photonic and plasmonic resonances, *Laser Photonics Rev.* **12**, 1700113 (2018).
- [60] D. Pook-Kolb, O. Birnholtz, J. L. Jaramillo, B. Krishnan, and E. Schnetter, Horizons in a binary black hole merger II: Fluxes, multipole moments and stability, [arXiv:2006.03940](https://arxiv.org/abs/2006.03940).
- [61] H. P. Nollert, Quasinormal modes of Schwarzschild black holes: The determination of quasinormal frequencies with very large imaginary parts, *Phys. Rev. D* **47**, 5253 (1993).
- [62] H. P. Baltes and E. R. Hilf, *Phys. Today* **30**, No. 8, 55 (1976).
- [63] M. Berger, *A Panoramic View of Riemannian Geometry* (Springer, Berlin, 2003).
- [64] W. Arendt, R. Nittka, W. Peter, and F. Steiner, *Weyl's Law: Spectral Properties of the Laplacian in Mathematics and Physics* (John Wiley & Sons, Ltd., New York, 2009), Chap. 1, pp. 1–71, [10.1002/9783527628025.ch1](https://doi.org/10.1002/9783527628025.ch1).
- [65] I. G. Moss, Can you hear the shape of a bell?: Asymptotics of quasinormal modes, *Nucl. Phys. B, Proc. Suppl.* **104**, 181 (2002).
- [66] J. Sjöstrand, Weyl law for semi-classical resonances with randomly perturbed potentials, No. 136 in *Mémoires de la Société Mathématique de France*, (Société Mathématique de France, France, 2014), [10.24033/msmf.446](https://doi.org/10.24033/msmf.446).
- [67] R. Froese, Asymptotic distribution of resonances in one dimension, *J. Differ. Equations* **137**, 251 (1997).
- [68] B. Simon, Resonances in one dimension and Fredholm determinants, *J. Funct. Anal.* **178**, 396 (2000).
- [69] L. Motl, An analytical computation of asymptotic Schwarzschild quasinormal frequencies, *Adv. Theor. Math. Phys.* **6**, 1135 (2002).
- [70] L. Motl and A. Neitzke, Asymptotic black hole quasinormal frequencies, *Adv. Theor. Math. Phys.* **7**, 307 (2003).
- [71] M. Maggiore, Physical Interpretation of the Spectrum of Black Hole Quasinormal Modes, *Phys. Rev. Lett.* **100**, 141301 (2008).
- [72] J. L. Jaramillo, R. P. Macedo, and B. Raffaelli, A Weyl's law for black holes (to be published).
- [73] V. Cardoso, M. Kimura, A. Maselli, E. Berti, C. F. B. Macedo, and R. McManus, Parametrized black hole quasinormal ringdown: Decoupled equations for nonrotating black holes, *Phys. Rev. D* **99**, 104077 (2019).
- [74] R. H. Price, Nonspherical perturbations of relativistic gravitational collapse. II. Integer-spin, zero-rest-mass fields, *Phys. Rev. D* **5**, 2439 (1972).
- [75] S. H. Tang and M. Zworski, Resonance expansions of scattered waves, *Commun. Pure Appl. Math.* **53**, 1305 (2000), <https://citeseerx.ist.psu.edu/viewdoc/summary?doi=10.1.1.23.6001>.
- [76] M. Ansorg and R. Panosso Macedo, Spectral decomposition of black-hole perturbations on hyperboloidal slices, *Phys. Rev. D* **93**, 124016 (2016).
- [77] R. Panosso Macedo, J. L. Jaramillo, and M. Ansorg, Hyperboloidal slicing approach to quasi-normal mode expansions: The Reissner-Nordström case, *Phys. Rev. D* **98**, 124005 (2018).
- [78] E. Gasperin and J. L. Jaramillo, QNM instability and weak formulations of the scattering problem (to be published).
- [79] R. Panosso Macedo and M. Ansorg, Axisymmetric fully spectral code for hyperbolic equations, *J. Comput. Phys.* **276**, 357 (2014).
- [80] G. Prony, Essai expérimental et analytique: Sur les lois de la dilatabilité, *J. Éc. Polytech. (Paris)* **22**, 24 (1795).
- [81] E. Berti, V. Cardoso, J. A. Gonzalez, and U. Sperhake, Mining information from binary black hole mergers: A comparison of estimation methods for complex exponentials in noise, *Phys. Rev. D* **75**, 124017 (2007).
- [82] For optimization, we select the signal at \mathcal{H} as the ring-down lasts longer than at \mathcal{S}^+ . Prony's method is applied for $\tau \in [6, 50]$, with $p = 8$, $L = 40$, $N = 401$ (Ref. [81]'s notation).

- [83] M. Ammon, S. Griener, A. Jimenez-Alba, R. P. Macedo, and L. Melgar, Holographic quenches and anomalous transport. *J. High Energy Phys.* **09** (2016) 131.
- [84] Beyond providing new QNM branch patterns as an “*a priori*” input for data analysis, it is tantalizing to compare with the historical developments prompted by Lorentz’ studies of high overtone asymptotics in Jeans radiation theory (see, e.g., [85]), which eventually led to the foundational notion of black body radiation in physics. Overtones encode information on small scales and their systematic study in the (perturbed) BH context could open unexpected connections with fundamental gravity physics.
- [85] M. Kac, Can one hear the shape of a drum? *Am. Math. Mon.* **73**, 1 (1966).